Author(s): Morgan, Matthew M.; Patrick, Evan A.; Rautiainen, J. Mikko; Tuononen, Heikki; Piers, Warren E.; Spasyuk, Denis M.

Title: Zirconocene-Based Methods for the Preparation of BN-Indenes : Application to the Synthesis of 1,5-Dibora-4a,8a-diaza-1,2,3,5,6,7-hexaaryl-4,8-dimethyl-s-indacenes

Year: 2017

Version:

Please cite the original version:

Morgan, M. M., Patrick, E. A., Rautiainen, J. M., Tuononen, H., Piers, W. E., & Spasyuk, D. M. (2017). Zirconocene-Based Methods for the Preparation of BN-Indenes : Application to the Synthesis of 1,5-Dibora-4a,8a-diaza-1,2,3,5,6,7-hexaaryl-4,8-dimethyl-s-indacenes. Organometallics, 36(14), 2541-2551. https://doi.org/10.1021/acs.organomet.7b00051

Zirconocene-based methods for the preparation of BN indenes: application to the synthesis of 1,5-dibora-4a,8a-diaza-1,2,3,5,6,7-hexaaryl-4,8-dimethyl-*s*-indacenes.

Matthew M. Morgan,[†] Evan A. Patrick,[†] J. Mikko Rautiainen,*[‡] Heikki M. Tuononen,[‡] Warren E. Piers,*[†] and Denis M. Spasyuk[§]

[†]Department of Chemistry, University of Calgary, 2500 University Drive N.W., Calgary, Alberta, T2N 1N4 [‡]Department of Chemistry, Nanoscience Center, University of Jyväskylä, P.O. Box 35, FI-40014 Jyväskylä, Finland and [§]Canadian Light Source Inc. 44 Innovation Boulevard, Saskatoon, Saskatchewan, Canada SK S7N 2V3

Supporting Information Placeholder

ABSTRACT: A method for the preparation of 3-bora-9aza-indene heterocycles based on zirconocene mediated functionalization of the *ortho*-CH bonds of pyridines has been developed and used to make two such compounds. Unlike other methods, the boron center in these heterocycles remains functionalized with a chloride ligand and so the compounds can be further elaborated through halide abstraction and reduction. The utility of the method was further demonstrated by applying it towards the preparation of 1,5-dibora-4a,8a-diaza BN analogues of the intriguing hydrocarbon *s*-indacene starting from 2,5-dimethylpyrazine. Gram quantities of one such compound was prepared and fully characterized, and both experimental and computational data is presented to compare its properties to those of the parent hydrocarbon *s*-indacene. These data indicate that the BN substituted derivative exhibits lowered aromaticity in relation to the hydrocarbon.

INTRODUCTION

The substitution of C-C with isoelectronic and isosteric BN building blocks within conjugated organic frameworks has been explored since the seminal work of Dewar, beginning in the late 1950s.[1,2] These early studies, informed by the prior discovery of borazine,[3] were motivated mainly by curiosity and shed light on the concept of aromaticity in conjugated systems. In the past decade, however, evaluating the effect of BN for CC substitution on the electronic properties of various conjugated hydrocarbon-based molecules,[4-16] polymers[17-20] and materials[21-26] has emerged as a primary goal of the field. Furthermore, the introduction of a significant dipole has implications for the BN analogues of hydrocarbons as biological agents.[27-31] There has therefore been a significant amount of activity in this field since its resurgence in the mid 2000's.[32-38]

A corollary of the interest in these molecules is the need for new synthetic routes to such species that are efficient, modular and scalable.[35] While much progress has been made, new methodologies are still of interest for preparing these materials and accessing BN frameworks for which current methods are not suited. Here we describe a zirconocene-based method for assembling 3-bora-9-aza-indene scaffolds[39-40] and its use to prepare 1,5-dibora-4a,8a-diaza BN analogues (**I**) of the intriguing "quasi aromatic" hydrocarbon *s*-indacene (**II**).[41-44]

RESULTS AND DISCUSSION

We have previously shown that zirconocycles are useful starting materials for the synthesis of boron containing heterocycles.[45-46] We hypothesized that by using well-established

Chart 1

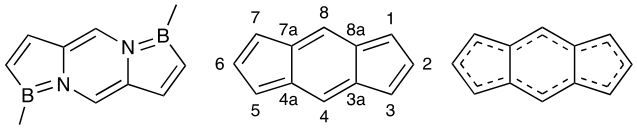

I **II-C_{2h}** **II-D_{2h}**

zirconocene chemistry in which the *ortho* C-H bonds of pyridine can be selectively functionalized,[47-49] these routes might be adaptable to preparing 3-bora-9-aza-indene functions with modular control over the substituents on the heterocyclic framework. Exploratory experiments (Scheme 1) showed that the zirconocene methyl cation generated by methide abstraction using $[Ph_3C][B(C_6F_5)_4]$[50] reacted readily with pyridine to eliminate methane and give the expected η^2-pyridyl cation **1•B(C_6F_5)$_4$**.[47] Insertion of diphenyl acetylene into the Zr–C bond was facile, selectively yielding the five-membered zirconacyclic cation **2•B(C_6F_5)$_4$**.[48] It was anticipated that reaction of this species with $PhBCl_2$ would yield the desired BN heterocycle, with "$[Cp_2ZrCl][B(C_6F_5)_4]$" as the by-product, but no reaction was observed between **2•B(C_6F_5)$_4$** and the haloborane under any conditions we explored. However, if the cation was neutralized with the more coordinating chloride anion to give **3**, the transmetalation reaction proceeded smoothly to yield the desired product (*vide infra*). The synthetic intermediates shown in Scheme 1 (**1•B(C_6F_5)$_4$**, **2•B(C_6F_5)$_4$**, and **3**) were characterized via comparison with known compounds[51] and via spectroscopic and structural characterization (see the Supporting Information). Although **3** was not isolated in

Scheme 1. Generation of BN-indene scaffolds via zirconocene chemistry.

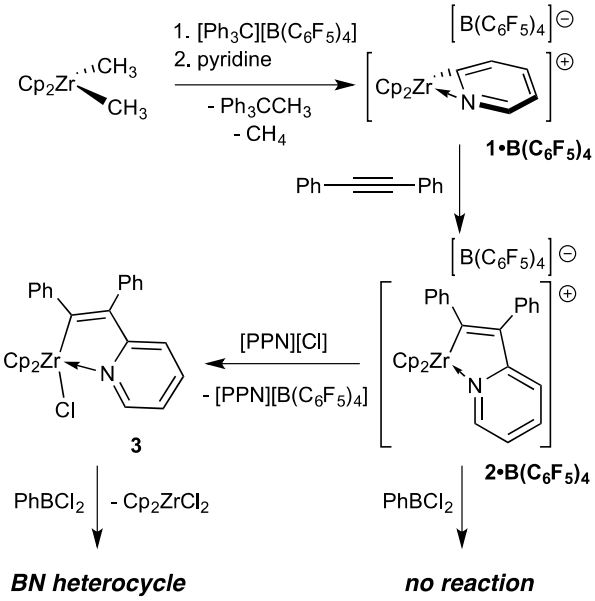

analytically pure form due to contamination with the [PPN][$B(C_6F_5)_4$] salt byproduct, a structure determination was possible on carefully picked crystals. Analysis of the Zr-C and Zr-N distances in cation **2•B(C_6F_5)$_4$** vs. neutral **3**, (Figure S1 in the Supporting Information) shows a significant lengthening of the bonds by 0.13–0.17Å in the latter; this, coupled with the lowered Lewis acidity of the zirconium center makes **3** more reactive towards the haloborane reagent.

Scheme 2. Two step generation of BN-indenes.

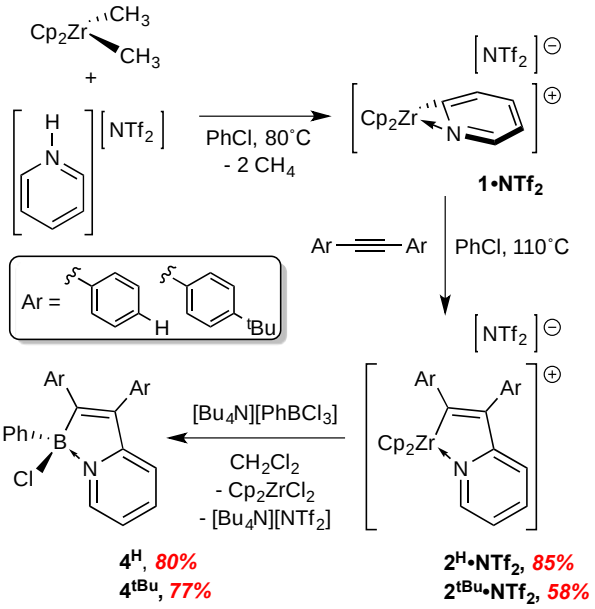

The need to switch from cationic to neutral zirconocene chemistry makes the route shown in Scheme 1 somewhat atom extravagant and so efforts were made to streamline the synthesis as much as possible. The protocol shown in Scheme 2 was developed and used to prepare the 3-bora-9-aza heterocycles **4^{H}** and **4^{tBu}** in a convenient, scalable (up to 5 grams) and high yielding two-step synthesis. In the first step, the η^2-pyridyl complex **1•NTf_2** was generated *in situ* via reaction of dimethylzirconocene and the triflimato pyridinium salt,[52] and used without isolation in further reactions with the diarylacetylenes shown. Unfortunately, the analogous triflate salt **1•OTf** could not be prepared, probably due to the higher coordinating tendencies[53] of OTf^- vs NTf_2^- in the $Cp_2Zr(CH_3)ETf_n$ products of protonolysis. Pyridine is unreactive toward the triflate derivative,[54] but for E = N, n = 2, the product zirconacycles **2^{H}•NTf_2** and **2^{tBu}•NTf_2** were isolated in good yields, the former on a multigram scale. Instead of using [PPN][Cl] as the chloride source, cations **2•NTf_2** were treated with [Bu_4N][$PhBCl_3$],[55] and the required neutral zirconocenes **3^{H}** and **3^{tBu}** were generated *in situ* in the presence of $PhBCl_2$ leading directly to the BN indene products **4^{H}** and **4^{tBu}** in high yield as shown in Scheme 2.[56,57-58]

This protocol provides an alternative, and potentially more versatile, route to these 3-bora-9-aza indenes to those reported by Murakami[39] and Wang[40] (Scheme 3). In the Murakami method, palladium catalysis converts the zwitterionic alkynylpyridinium borate substrates to the BN indenes in a high-yielding reaction that allows for hydrocarbyl substituents on the pyridinium ring, and some variation in the aryl substituents on the borate. In the Wang synthesis, an unusual *trans* hydroboration is observed when the 2-alkynylpyridine substrates are treated with stoichiometric 9-borabicyclo[3.3.1]nonane (9-BBN). Here, the yields are somewhat lower and the R group is restricted to being an aryl group or a silyl substitutent. In both previous methods, the boron atom of the BN indene ring is substituted by two aryl or alkyl groups, making further chemical derivatization at the boron center difficult.

Scheme 3. Murakami and Wang syntheses of BN-indenes.

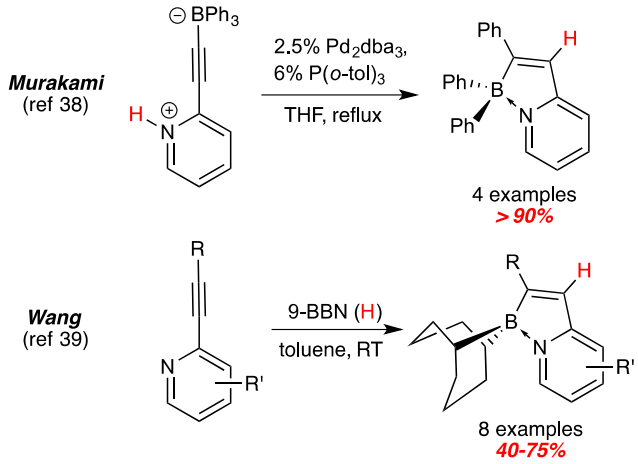

Compounds **4^{R}** are isolable as air and moisture tolerant yellow powders by filtering the reaction mixtures through a plug of silica to remove the byproducts. Vacuum-line techniques are not required for these manipulations. The two derivatives were fully characterized by spectroscopy and via an X-ray structural analysis on **4^{H}** (*vide infra*). In addition to the expected resonances in the ^{1}H NMR spectra, the compounds are characterized by ^{11}B chemicals shifts of 5.8 (**4^{H}**) and 6.3 (**4^{tBu}**) ppm, consistent with four-coordinate, neutral boron centers. Like the previous examples reported, compound **4^{H}** exhibits blue fluorescence at 481 nm on excitation at its lowest energy absorption band of 369 nm (ε = 9.4 x 10^3 M^{-1} cm^{-1}) with an observed Stokes shift of 112 nm (6310 cm^{-1}). Spin-coating a film of the compound onto a glass substrate shows that the

solid also fluoresces, albeit with a slightly reduced Stokes shift of 99 nm (5517 cm^{-1}). The lowest energy absorbance has been attributed to a π-π* transition from the HOMO, based primarily on the six-membered ring, to the LUMO which is largely associated with the five-membered ring.[40]

Potential variation in the diaryl acetylene employed, the $ArBX_2$ reagent utilized, and substitution on the pyridyl component makes this route a modular strategy for assembling 3-bora-9-aza indene ring systems. In addition, and distinct from the previously reported methods, in this route the boron retains a halogen function in the products, allowing for further derivatization of the core framework. For example, as shown in Scheme 4, this halide can be exchanged for other anions via abstractive protocols, or removed via two-electron reduction to form a BN-indenylide anion. Treatment of $\mathbf{4^H}$ with trimethylsilyl triflamide, $TMSNTf_2$, rapidly produces TMSCl and a new 3-bora-9-azaindene, $\mathbf{5^H}$, in which the NTf_2 anion has replaced the chloride ion. The X-ray structure of $\mathbf{5^H}$ was determined (see Figure S2 in the Supporting Information) and despite some disorder in the NTf_2 anion, it is apparent that in the solid state it remains coordinated to the boron center through one of the oxygen atoms (B1-O1 = 1.565(6)Å). The bond distances within the BN-indene ring of $\mathbf{5^H}$ do not differ significantly from those seen in $\mathbf{4^H}$ (Figure 1) and the ^{11}B NMR resonance for $\mathbf{5^H}$ (10.5 ppm) compared to $\mathbf{4^H}$ (5.8 ppm) suggests, despite the slight downfield shifted, that the borenium ion character in this compound is low. Still, in the ^{19}F NMR spectrum, the CF_3 groups appear as a single resonance even at low temperatures, suggesting some lability in the anion and the potential for $\mathbf{5^H}$ to serve as a borocation[59] synthon.

Scheme 4. Reactions of $\mathbf{4^H}$.

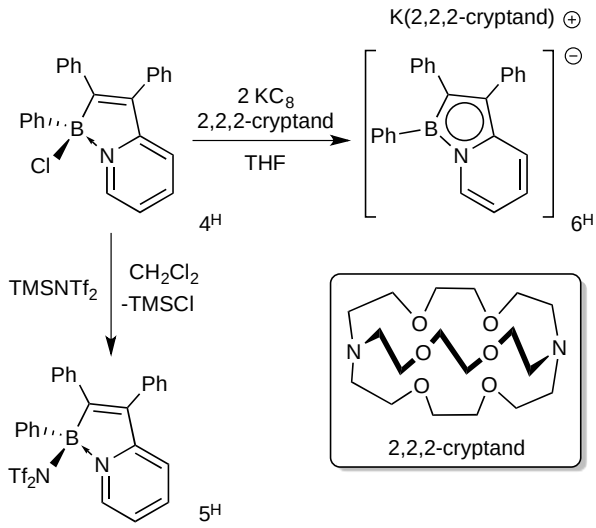

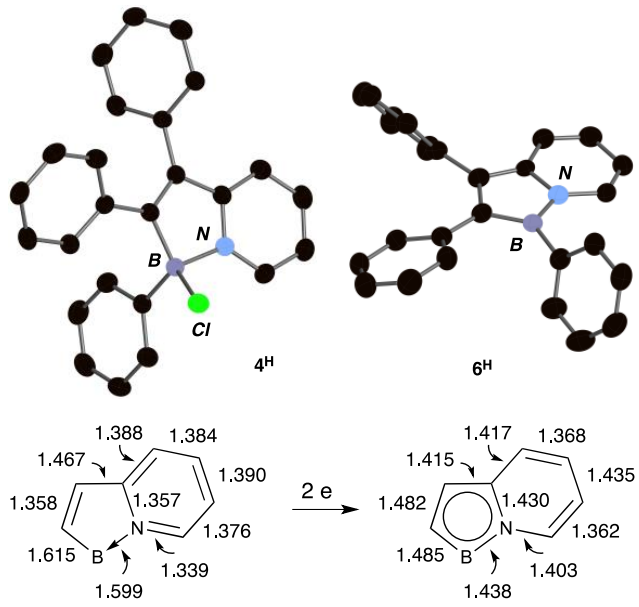

Figure 1. Thermal ellipsoid (50%) diagrams of the molecular structures of $\mathbf{4^H}$ (left) and $\mathbf{6^H}$ (right); Hydrogen atoms have been removed for clarity in both structures and for $\mathbf{6^H}$, the $[(2,2,2\text{-cryptand})K]^+$ is omitted. Below each structure, the bond distances for the bonds of the 3-bora-9-aza rings are given; for clarity, the e.s.d. values are omitted, but none are greater than 4.

Electrochemical measurements on $\mathbf{4^H}$ suggest that it can be reduced by two electrons, using strong reducing agents, to produce the BN analogue of the indenyl anion. Accordingly, treatment of THF solutions of the chloroborane with KC_8 led to a rapid yellow to red color change and after workup, the potassium salt could be isolated as an orange powder. Use of 2,2,2-cryptand allowed us to obtain crystals suitable for X-ray diffraction, but for reactivity studies, the cryptand is not necessary. The structures of both $\mathbf{4^H}$ and $\mathbf{6^H}$ are depicted in Figure 1 for easy comparison. It is apparent that the boron center goes from tetrahedral to planar and this is reflected in the downfield shift of the boron resonance for $\mathbf{6^H}$ to 24.5 ppm. A comparison of the bond distances within the fused BN framework shows that in $\mathbf{4^H}$ there is bond alternation in the five-membered ring, while in the six-membered pyridyl ring the congruent distances indicate delocalization. The situation is reversed in the 10π anion $\mathbf{6^H}$, where bond equalization is apparent in the BN containing ring, while localization occurs in the pyridyl ring. This is supported by Nucleus Independent Chemical Shift (NICS) computations using Density Functional Theory (DFT), which show that the five membered ring is aromatic with NICS(0) and NICS(1) values of –13.1 and –11.1 respectively, while the six membered ring is non-aromatic with NICS values near zero (see Table S11 in the Supporting Information).

Having demonstrated the efficacy of the zirconocene-based methodology for assembling 3-bora-9-aza indenes, we sought to apply it to the synthesis of a new BN heterocyclic framework. *s*-Indacene (**II**, Chart 1) is an interesting conjugated hydrocarbon due to its ambiguous aromaticity. Although it is a 12 π system, and therefore formally antiaromatic, experimental[41, 60-61] and computational studies[42, 62-63] show that there is significant carbon–carbon bond equalization on the perimeter of the molecule, leading to its description as a "quasi-aromatic" system. These studies thus suggest that it assumes a D_{2h} instead of a C_{2h} structure (Chart 1) in which the C=C bonds are more localized. Nonetheless, the synthesis of *s*-indacene derivatives is a challenge,[43] and must include sterically bulky substituents in the 1,3,5,7-positions,[41] or electron donating groups in the 4,8-positions[64] to prevent decomposition pathways that arise because of the considerable diradical character of the ground state D_{2h} structure.[62] Suitably substituted derivatives can be reduced by one[65] or two[66] electrons and have promise as structural subunits in conductive organic materials.[67-68] Readily accessible BN-*s*-indacenes,[69,70] therefore, may be of interest for incorporation into devices that utilize such materials, but are also of fundamental significance in

Scheme 5. Synthesis of 1,5-dibora-4a,8a-diaza-1,2,3,5,6,7-hexaaryl-4,8-dimethyl-*s*-indacenes.

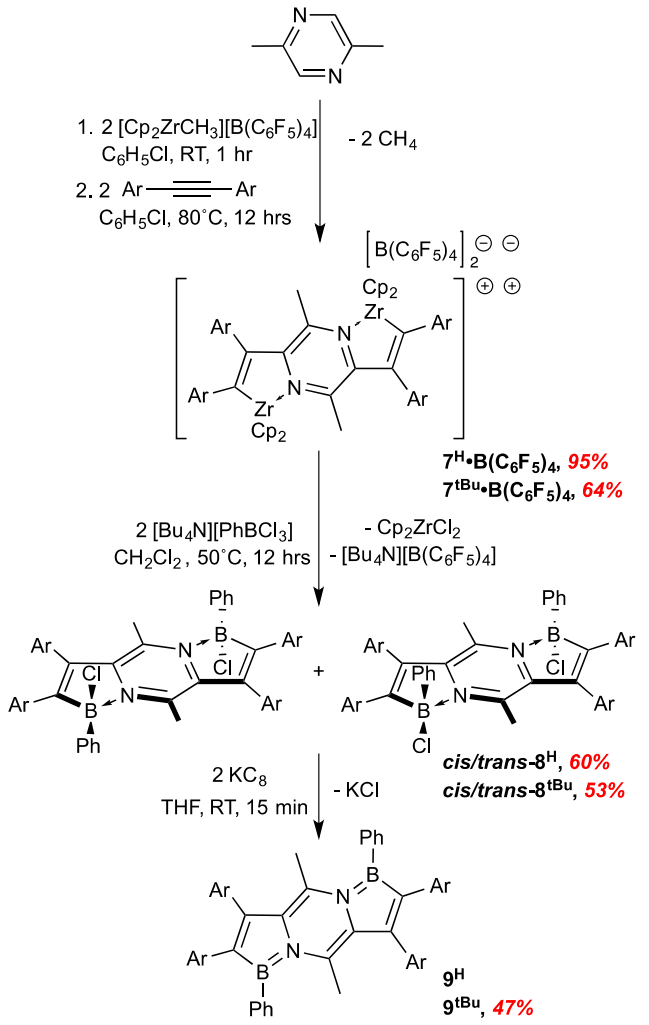

addressing the effect of BN substitution on bond delocalization within the cyclic framework.

Accordingly, we sought to apply our methodology to this problem. In order to direct the synthesis to the desired 1,5-dibora-4a,8a-diaza BN-indacene, 2,5-dimethylpyrazine was selected as the substrate for C–H activation with $[Cp_2ZrCH_3]^+$ (Scheme 5). Unfortunately, the pyrazine could not be doubly protonated to prepare a suitable NTf_2 salt and so $[Cp_2ZrCH_3][B(C_6F_5)_4]$ had to be employed for this synthesis for direct reaction with the pyrazine. The dimeric η^2-pyridyl dication expected from double C–H activation of the pyrazine substrate (not shown in Scheme 5) formed smoothly, and in the optimized syntheses was used without isolation to generate the two zirconacycles **7^{H}•B(C$_6$F$_5$)$_4$** and **7^{tBu}•B(C$_6$F$_5$)$_4$** in excellent yields as deep purple solids on scales of up to 2 grams. Both compounds have been fully characterized, including via X-ray crystallography in the case of **7^{H}•B(C$_6$F$_5$)$_4$** (see Figure S3 in the Supporting Information). The structure is similar in nature to that found for **2^{H}•B(C$_6$F$_5$)$_4$** and the purple color in comparison to the orange hue of **2^{H}•B(C$_6$F$_5$)$_4$** is presumably due to the more extended conjugation in **7^{H}•B(C$_6$F$_5$)$_4$**. As shown in Scheme 5, the zirconacycles were carried forward to the pink colored boracycles **8^{R}** via treatment with $[Bu_4N][PhBCl_3]$; compounds **8^{R}** are produced as essentially 1:1 mixtures of the *cis* and *trans* isomers as defined by the disposition of the substituents on boron across the plane of the polycyclic framework. The isomers are distinguishable by NMR spectroscopy, and they can be enriched by careful fractional crystallization methods because the *cis* isomer is more soluble in CH_2Cl_2/hexanes mixtures than the *trans*. In this way, the molecular structures of both *cis*-**8^{H}** and *trans*-**8^{H}** were determined (Figure S4 in the Supporting Information) and the nature of the isomers produced in this reaction confirmed. In terms of bond distances within the heterocyclic framework, the two isomers are very similar, and since separation of these isomers is not necessary for the next step, they will not be discussed in detail here. Interestingly, a *cis*-enriched sample of **8^{H}** (95:5) could be equilibrated back to a 50:50 mixture by heating to 50 °C for several hours, indicating that this is the thermodynamic ratio of the *cis* and *trans* isomers. The mechanism of equilibration is unknown, but involvement of borenium ions[59] accessible via chloride dissociation is the most likely scenario.

Compounds **8^{R}** serve as ideal precursors to the target 1,5-dibora-4a,8a-diaza BN-indacenes via reduction by two electrons using KC_8. These reactions proceed efficiently at room temperature in THF. For the reduction of *cis/trans*-**8^{H}**, the product **9^{H}** precipitates as a yellow powder from the reaction mixture and was found to be sparingly soluble in all common solvents. It was therefore difficult to purify and obtain NMR data on this species. A molecular structure with poor bond precision was obtained and established the connectivity of the structure conclusively. The compound **9^{tBu}**, however, was more well-behaved and fully characterized by all the usual means. A resonance at 42.3 ppm was observed in the ^{11}B NMR spectrum, and the patterns of resonances in both the ^{1}H and

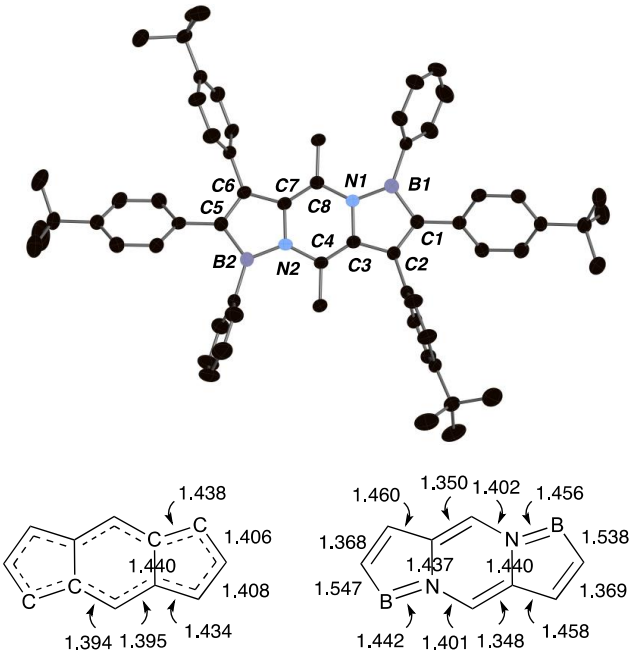

Figure 2. Thermal ellipsoid (50%) diagrams of the molecular structure of **9^{tBu}**; Hydrogen atoms have been removed for clarity. Below the structure, the bond distances for the bonds within the tricyclic ring system are given, along with those for the parent hydrocarbon as its 1,3,5,7-*tert*-butyl-substituted derivative;[61] for clarity, the e.s.d. values are omitted, but none are greater than 5.

^{13}C NMR spectra were fully consistent with the proposed structure. The compounds were not stable on exposure to ambient atmosphere, with both solutions and solid samples returning to a dark pink color in the presence of O_2/H_2O. The nature of the products was not determined.

Single crystals of **9^{tBu}** were obtained from THF/pentane and the molecular structure is depicted in Figure 2. The $C_8B_2N_2$ heterocyclic ring system is planar, with the range of deviation from the least squares plane defined by these atoms being 0.008–0.070 Å. The bond distances within the tricyclic framework are depicted below the structure, along with the values found for 1,3,5,7-*tert*-butyl-*s*-indacene (**II^{tBu}**).[61] It can be seen that the bond alternation in **9^{tBu}** is pronounced in comparison to the delocalization observed in the all-carbon tricycle. In particular, short B–N distances of 1.442(5) and 1.456(5) Å are suggestive of double-bond character, and the distances of 1.369(5) Å for C1–C2 and 1.368(5) Å for C5–C6 indicate localized C=C bonds. DFT level NICS computations are consistent with this picture, as the NICS(1) and NICS(0) values for both the five-membered ring (-3.2; -2.0) and the central six-membered ring (-0.3, 1.4) indicate that they are nonaromatic (Table S11 in the Supporting Information). Thus, in comparison, the 12-π BN-*s*-indacene ring system is significantly more localized than that in the all-carbon analogue.

In order to further compare the electronic structures of **9^{R}** and *s*-indacene, gauge-including magnetically induced current (GIMIC) calculations were performed at the DFT level.[71-72] In short, GIMIC analysis allows for the determination and visualization of magnetically induced diatropic (clockwise) and paratropic (anti-clockwise) ring currents (Figure 3) that are associated with aromaticity and antiaromaticity, respectively.[72] Specifically, for aromatic molecules, diatropic current on the outside of the rings (depicted by blue surface in Figures 3a and 3d) dominates over the paratropic current (red surface in Figures 3a and 3d) that lies mostly inside the rings, while the relative strengths of the currents are reversed for antiaromatic molecules. For comparative purposes, a net ring current can be calculated for each ring in the molecule by averaging the net currents of individual bonds in the ring (calculated by integrating the diatropic and paratropic currents through a cross section of the bond).

In the case of *s*-indacene, the **II-*D*$_{2h}$** symmetric structure with a broken symmetry singlet ground state was calculated to be the global minimum, in agreement with the diradical character of **II**.[62] Although the **II-*C*$_{2h}$** structure was found to be a local minimum 3.1 kcal mol^{-1} higher in enthalpy than **II-*D*$_{2h}$**, it was nevertheless used in the GIMIC analysis to represent a formally anti-aromatic reference system.[73] Furthermore, instead of employing **9^{H}** or **9^{tBu}** in the GIMIC analysis, the parent 12-π BN-*s*-indacene **I^{H}** (Figure 3e) was used to simplify the interpretation of results.

For **II-*C*$_{2h}$**, the magnetically induced current profiles across inequivalent bonds (Figure 3c) and integrated current contributions (Table 1) indicate that paratropic (negative) contributions to the net current are much stronger than diatropic contributions for all of the bonds apart from the bond connecting the five- and six-membered rings. Consequently, the net ring currents calculated as averages of the integrated current strengths of individual bonds were found to be strongly paratropic for both the five (–7.6 nA T^{-1})- and six-membered (–5.6 nA T^{-1}) rings, in line with the 12-π antiaromatic nature of the structure. By comparison, the current strength profiles of **I^{H}** bonds (Figure 3f) indicate comparable contributions from both paratropic and diatropic parts of the magnetically induced current that result in weak net ring currents for both the five (2.6 nA T^{-1})- and six-membered rings (–1.0 nA T^{-1}). The weak net currents are consistent with the non-aromatic nature inferred for **9^{tBu}** from NICS calculations and bond distance analysis. The observed change towards nonaromaticity upon BN for CC substitution is reminiscent of the decrease in the degree of aromaticity in 1,2-dihydro-1,2-azaborine[74] and BN substituted fused polyaromatic hydrocarbons[75] compared to their all-carbon analogues.

From the individual contributions of diatropic and paratropic currents to the net current (Table 1), the GIMIC analysis shows that the strengths of diatropic bond currents increase only slightly going from **II-*C*$_{2h}$** to **I^{H}** whereas the paratropic currents decrease significantly. The analysis also reveals distinct fluctuations in the strengths of diatropic and paratropic currents going from one bond to the next, but the net currents across the perimeter bonds of a particular ring in **II-*C*$_{2h}$** or **I^{H}** stay roughly the same regardless of the atoms involved in the bonds. This demonstrates that the BN for CC substitution in **I^{H}** affects the net currents across all the bonds in the molecule and the observed differences in ring currents between **II-*C*$_{2h}$** and **I^{H}** are not simply due to localized contributions from the BN heteroatom bonds.

Table 1. Integrated diatropic and paratropic magnetically induced current contributions to the net current strengths in inequivalent bonds of **II-*C*$_{2h}$** and **I^{H}** [in nA T^{-1}]. See Figures 3b and 3e, respectively, for color coding of bonds.

	Bond		Diatropic	Paratropic	Total
II-*C*$_{2h}$	■	C-C	7.8	–16.6	–8.8
	■	C-C	12.1	–11.3	0.8
	■	C-C	6.8	–16.4	–9.6
	■	C-C	6.6	–15.4	–8.8
	■	C-C	7.7	–17.3	–9.6
	■	C-C	7.0	–16.9	–9.9
	■	C-C	5.8	–15.7	–9.9
I^{H}	■	C-N	8.4	–8.2	0.2
	■	C-N	6.8	–10.3	–3.5
	■	B-N	9.9	–5.6	4.3
	■	C-C	9.3	–8.9	0.4
	■	C-C	10.6	–6.5	4.1
	■	C-C	9.8	–5.5	4.3
	■	C-C	12.9	–8.7	4.2

The differences observed in the GIMIC analysis of **II-*C*$_{2h}$** and **I^{H}** are also borne out in the electronic structure of the two compounds. The UV–vis spectrum of **9^{tBu}** exhibits two main absorptions at 314 and 458 nm, the latter being ascribed to a HOMO to LUMO excitation by TDDFT analysis (Table S12 in the Supporting Information). Cyclic voltammetry (CV) measurements showed that the compound undergoes two irreversible reductions at –2.28 V and –2.67 V (vs Fc/Fc^{+}) and an irreversible oxidation at –0.73 V (Figure S25 in the Supporting

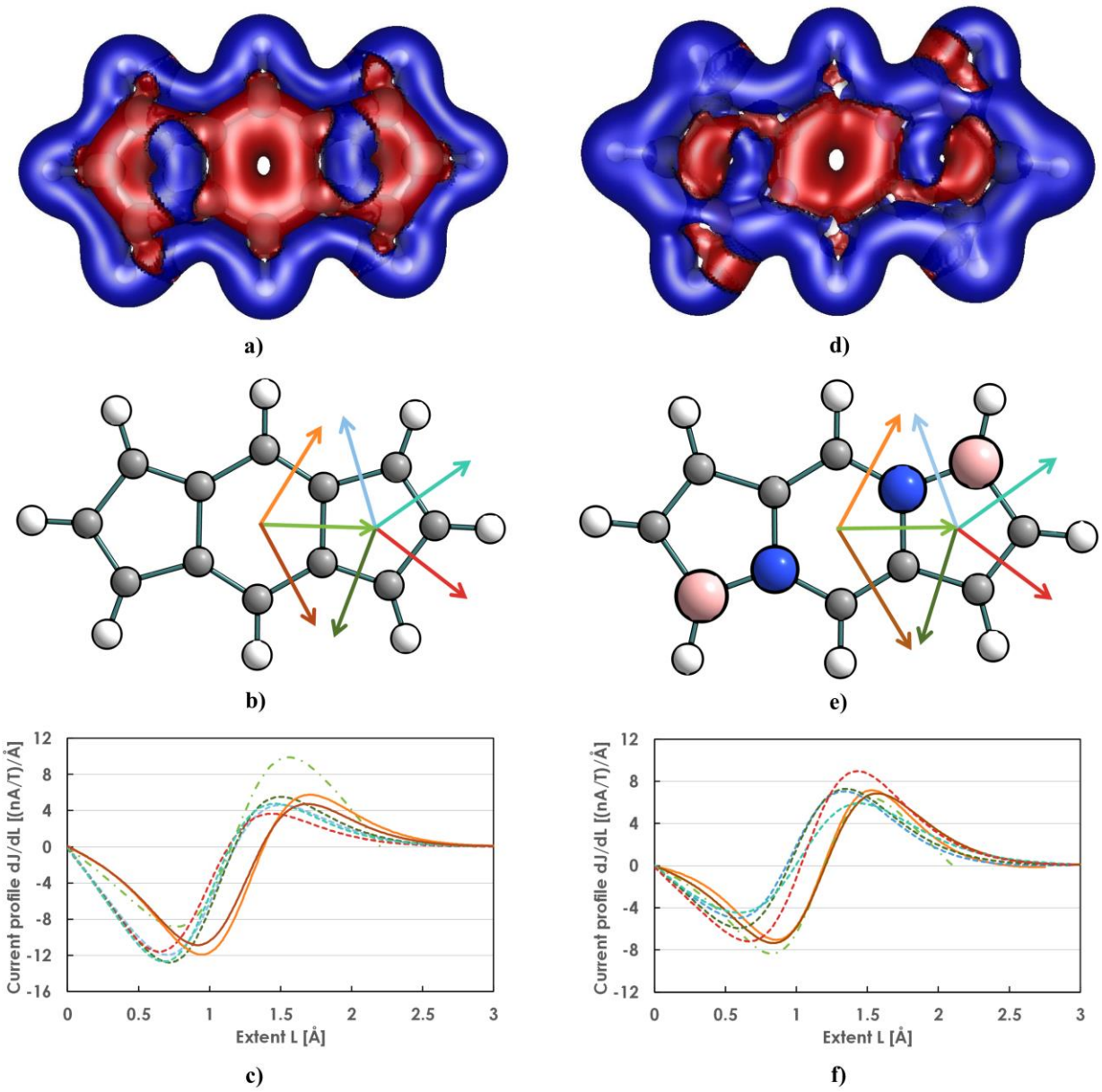

Figure 3. Results from GIMIC analyses for **II-C$_{2h}$** (left) and **I^{H}** (right). a) and d): Isosurface (0.015) of the signed modulus of the calculated magnetically induced current density (blue, diatropic current; red, paratropic current); b) and e): color coding for inequivalent bonds; and e) and f): current strength profiles across the bonds.

Information). From the intersection of the normalized UV–vis absorption and emission data, a HOMO/LUMO gap of 2.43 eV was obtained, which compares reasonably well with the computed value of 3.44 eV obtained from the TDDFT analysis. This gap is substantially larger than that calculated for the hydrocarbon **II^{tBu}** (2.76 eV), which is more readily and reversibly reduced to its radical anion[65] or dianion[66] than the BN-*s*-indacene compounds reported here. NICS computations on the putative dianion of **9^{tBu}** indicated that this 14-π species exhibits levels of aromaticity in the flanking five-membered rings similar to those of **6^{H}** (Table S11 in the Supporting Information), but it is 26.3 kcal mol^{-1} less stable than the neutral species in the gas phase. Although such an energy difference could be offset by anion–cation interactions in the solid state, attempts to chemically reduce **9^{tBu}** with KC_8 or potassium naphthalenide did not lead to isolable products. This is attributed to the apparent instability of reduced **9^{tBu}** seen in CV measurements, presumably due to the high energy LUMO of **9^{tBu}**. Interestingly, the anion **6^{H}** is highly reactive towards electrophiles, and it may be that the dianion of **9^{tBu}** is even more reactive and also a strong reducing agent. Further studies are underway to explore this reactivity.

CONCLUSIONS

This study reports a scalable new method for assembling BN heterocycles using established zirconocene-mediated pyridyl C–H functionalization chemistry. The methodology was optimized in the preparation of examples of 3-bora-9-aza-indenes and then applied to the more interesting 1,5-dibora-4a,8a-diaza BN analogues of the unique hydrocarbon *s*-indacene, which were fully characterized using spectroscopic, structural and computational tools. These investigations reveal that the BN substitution favors a more localized bonding framework, as would be found in the C_{2h} isomer of *s*-indacene,

which has been shown to be less favored than the more delocalized D_{2h} isomer. The BN-substituted material also features a larger HOMO–LUMO gap than the all-carbon framework.

EXPERIMENTAL SECTION

General. All experiments were performed under a purified argon atmosphere either using a MBraun Unilab glove box or a double-manifold high-vacuum line following standard techniques, unless otherwise specified. Hexanes, pentane, diethyl ether and tetrahydrofuran were dried and purified using a Grubbs/Dow solvent purification system and stored in 500ml thick-walled Kontes flasks over sodium/benzophenone ketal. Dichloromethane and chlorobenzene were stored in the same manner except for being dried over calcium dihydride instead of sodium/benzophenone ketal. All dried solvents were degassed and vacuum-distilled prior to use. All other commercially available starting materials were used without further purification. Compounds **1•B(C$_6$F$_5$)$_4$** and **2•B(C$_6$F$_5$)$_4$** were prepared as previously reported.[1] The reagents pyridinium triflamide[52] and tetrabutylammonium trichlorophenyl borate[55] were prepared by literature methods. NMR spectra were obtained using either a Bruker RDQ-400, Bruker Ascend-500, or Bruker Avance-600 MHz NMR spectrometer with solvent peaks referenced to tetramethylsilane as an internal standard for ^{1}H and ^{13}C. UV–Vis fluorescence data was collected using a Horiba FluoroMax-4 spectrometer. Cyclic voltammetry was collected with a CHI660D potentiostat. The bulk purity of synthesized compounds reported was assessed by elemental analysis on the batch of compound the yield is reported for, unless otherwise specified.

Synthesis of 2^{H}•NTf$_2$. A 100 ml round bottom flask was charged with pyridinium triflamide (2.545 g, 7.06 mmol), dimethylzirconocene (1.776 g, 7.06 mmol), PhCl (25 ml), and a Teflon stirbar, immediately producing a yellow solution with effervescence. The flask was then attached to a reflux condenser apparatus under flow of argon creating an open system to accommodate the loss of methane, and the mixture was stirred for 1.5 h. The mixture was then heated at 80 °C for 24 h yielding an amber solution. A slight excess of diphenylacetylene (1.385 g, 7.77 mmol) was then added and the mixture heated at 110 °C for 24 h producing an orange solution. Pentane (25 ml) was then vacuum-transferred into the flask with stirring, producing an orange precipitate, and the supernatant was decanted off via cannula transfer. The solid was then washed with pentane again (2 × 15 ml), after which it was dried *in vacuo*, yielding the product **2^{H}•NTf$_2$** as an orange solid (4.549 g, 6.00 mmol, 85%). Crystals suitable for X-ray were grown from a solution of **2^{H}•NTf$_2$** dissolved in PhCl and layered with pentane at –35 °C. ^{1}H NMR (500 MHz, Toluene-d_8) δ 8.53 (ddd, *J* = 5.9, 1.7, 0.8 Hz, 1H, Py-**H**), 7.07 – 7.02 (m, 2H, Ar-**H**), 6.96 – 6.90 (m, 3H, Ar-**H**), 6.87 (ddd, *J* = 8.1, 7.4, 1.7 Hz, 1H, Py-**H**), 6.85 – 6.82 (m, 2H, Ar-**H**), 6.78 – 6.71 (m, 2H, Py-**H** and 1× Ar-**H**), 6.70 (ddd, *J* = 8.1, 1.5, 0.8 Hz, 1H, Py-**H**), 6.68 – 6.64 (m, 2H, Ar-**H**), 6.01 (s, 10H, 2 × Cp). ^{13}C NMR (126 MHz, Toluene-d_8) δ 211.61, 164.38, 150.13 (**C**-H$_a$), 149.60, 141.92, 140.84 (**C**-H$_c$), 139.70, 130.50, 128.47, 128.01, 126.97, 125.94, 124.84, 123.68, 120.85, 120.53 (q, *J* = 321.5 Hz, -**C**F$_3$), 114.63 (2 × Cp) .^{19}F NMR (471 MHz, Toluene-d_8) δ –79.31. Elemental analysis calculated for $C_{31}H_{24}F_6N_2O_4S_2Zr$ (%):C, 49.13; H, 3.19; N, 3.70. Found: C, 48.77; H, 3.52; N, 3.69.

Synthesis of 2^{tBu}•NTf$_2$. A 100 ml thick-walled glass vessel was charged with pyridinium triflamide (143 mg, 0.40 mmol) and dimethylzirconocene (100 mg, 0.40 mmol), PhCl (25 ml), and a Teflon stirbar, immediately producing a yellow solution with effervescence. The headspace of the vessel was evacuated, and the mixture was stirred for 1.5 h. The headspace was evacuated a second time, and the mixture was heated at 80 °C for 24 h yielding a colorless solution. A slight excess of 1,2-bis(4-(tert-butyl)phenyl)ethyne (131 mg, 0.45 mmol) was then added and the mixture heated at 110 °C for 21 h, producing a red solution. The mixture was then transferred to a 50 ml two-necked round-bottom flask, to which pentane (25 ml) was vacuum-transferred, producing an orange precipitate. The supernatant was decanted off via cannula transfer, and the solid washed with additional pentane (2 × 10ml). The solid was then dried *in vacuo*, yielding the product **2^{tBu}•NTf$_2$** as an orange solid (201 mg, 0.23 mmol, 58%). ^{1}H NMR (500 MHz, Toluene-d_8) δ 8.65 (dt, *J* = 5.6, 1.2 Hz, 1H), 7.17 – 7.11 (m, 2H), 6.99 (d, J = 8.4 Hz, 2H), 6.82 (d, J = 8.2 Hz, 2H), 6.81 – 6.77 (m, 2H), 6.71 – 6.64 (m, 3H), 5.97 (s, 10H), 1.19 (s, 9H), 1.15 (s, 9H). ^{13}C NMR (126 MHz, Toluene-d_8) δ 212.20, 165.09, 150.53, 149.42, 147.73, 147.29, 142.07, 140.57, 130.33, 128.24, 125.98, 125.16, 123.56, 120.56, 120.37 (q, *J* = 321 Hz, -CF$_3$), 114.08, 34.48, 34.24, 31.34, 31.32. ^{19}F NMR (471 MHz, Toluene-d_8) δ –79.28. Elemental analysis calculated for $C_{39}H_{40}F_6N_2O_4S_2Zr$ (%):C, 53.84; H, 4.63; N, 3.22. Found: C, 53.55; H, 4.52; N, 3.28.

Synthesis of 4^{H}.

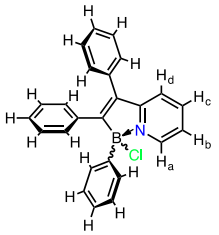

A 50 ml round-bottom flask was charged with **2^{H}•NTf$_2$** (248 mg, 0.33 mmol), [nBu$_4$N][PhBCl$_3$] (144 mg, 0.33 mmol), dichloromethane (15 ml), and a Teflon stirbar, producing an orange solution. The mixture was stirred for 16 h, producing a yellow solution. The mixture was then run through a silica/dichloromethane plug under atmospheric conditions, where a faint yellow band passed through and was collected. The solvent of the collected solution was then removed *in vacuo*, yielding the product as a yellow powder (99 mg, 0.26 mmol, 79%). Crystals suitable for X-ray study were grown from a solution of **4^{H}** dissolved in dichloromethane and layered with pentane at –35 °C. ^{1}H NMR (500 MHz, Methylene Chloride-d_2, 295K) δ 8.36 (dt, *J* = 5.7, 1.2 Hz, 1H **H$_a$**), 7.95 (td, *J* = 7.9, 1.5 Hz, 1H **H$_c$**), 7.58 – 7.50 (m, 2H, Ar-**H**), 7.52 – 7.44 (m, 2H, Ar-**H**), 7.47 – 7.39 (m, 1H, Ar-**H**), 7.42 – 7.35 (m, 3H, **H$_d$** + 2× Ar-**H**), 7.31 (ddd, *J* = 7.2, 5.7, 1.2 Hz, 1H, **H$_b$**), 7.30 – 7.17 (m, 5H, Ar-**H**), 7.15 – 7.04 (m, 3H, Ar-**H**). ^{13}C NMR (126 MHz, Methylene Chloride-d_2) δ 168.76, 160.47, 144.60, 143.44 (C-H$_a$), 142.98 (C-H$_c$), 138.06, 135.77, 135.24, 132.27, 130.13, 129.95, 129.50, 128.37, 128.04, 127.99, 127.82, 127.39, 121.80 (C-H$_b$), 119.69 (C-H$_d$). ^{11}B NMR (128 MHz, Methylene Chloride-d_2) δ 5.79 (br s). Elemental analysis of $C_{25}H_{19}BClN$ Calcd. (%):C, 79.08; H, 5.04; N, 3.69. Found: C, 78.88; H, 5.13; N, 3.56.

Synthesis of 4^{tBu}.

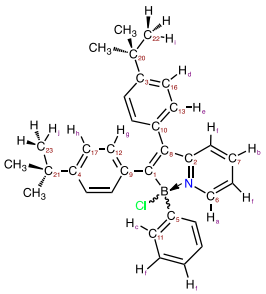

A 50 ml round-bottom flask was charged with **2^{tBu}•NTf$_2$** (100 mg, 0.12 mmol), [nBu$_4$N][PhBCl$_3$] (50 mg, 0.12 mmol) and dichloromethane (15 ml), producing an orange solution. The mixture was stirred for 41 h, producing a yellow/green solution. The mixture was then run through a silica/dichloromethane plug under atmospheric conditions, where a faint yellow/green band passed through and was collected. The solvent of the collected solution was then removed *in vacuo*, yielding the product as a yellow/green powder (43 mg, 0.09 mmol, 77%). ^{1}H NMR (500 MHz, Methylene Chloride-d_2) δ 8.30 (ddd, *J* = 5.8, 1.5, 0.9 Hz, 1H, **H$_a$**), 7.91 (ddd, *J* = 8.2, 7.4, 1.6 Hz, 1H, **H$_b$**), 7.56 (dt, *J* = 6.8, 1.5 Hz, 2H, **H$_c$**), 7.55 – 7.51 (m, 2H, **H$_d$**), 7.35 – 7.30 (m, 2H, **H$_e$**), 7.30 – 7.22 (m, 5H, **H$_f$**), 7.22 – 7.19 (m, 2H, **H$_g$**), 7.13 – 7.08 (m, 2H, **H$_h$**), 1.40 (s, 9H, **H$_i$**), 1.21 (s, 9H, **H$_j$**).^{13}C NMR (126 MHz, Methylene Chloride-d_2) δ 167.38 (C$_1$), 161.09 (C$_2$), 151.49 (C$_3$), 151.17 (C$_4$), 145.19 (C$_5$), 143.14 (C$_6$), 142.76 (C$_7$), 135.17 (C$_8$), 134.72 (C$_9$), 132.71 (C$_{10}$), 132.23 (C$_{11}$), 130.15 (C$_{12}$), 129.63 (C$_{13}$), 128.06, 127.35, 126.59 (C$_{16}$), 124.99 (C$_{17}$), 121.40, 119.65, 35.02 (C$_{20}$), 34.79 (C$_{21}$), 31.51 (C$_{22}$), 31.25 (C$_{23}$). ^{11}B NMR (161 MHz, Methylene Chloride-d_2) δ 6.32. HRMS (EI-TOF): *m*/*z* [M$^+$] Calcd for

$C_{33}H_{35}B^{35}ClN$ 491.2551; Found 491.2557. [M^+] Calcd for $C_{33}H_{35}B^{37}ClN$ 493.2522; Found 493.2569.

Synthesis of 5^H. Chloroborane $\mathbf{4^H}$ (50 mg, 0.132 mmol) was taken up in 5 ml of CH_2Cl_2, and to this a solution of $TMSNTF_2$ (47 mg, 0.132 mmol) in CH_2Cl_2 was added dropwise. As the solution of $TMSNTf_2$ was added the solution turned from pale yellow colour to darker yellow. The reaction was stirred for 30 min at room temperature, at which point volatiles were removed under vacuum, and pentane (30 ml) was added to the remaining solid. This suspension was then filtered in a swivel-frit apparatus, yielding a pale yellow solid, compound $\mathbf{5^H}$ (55 mg, 0.088 mmol, 67%).^{1}H NMR (500 MHz, Methylene Chloride-d_2) δ 8.29 (d, J = 5.7 Hz, 1H), 8.13 (td, J = 7.9, 1.5 Hz, 1H), 7.57 – 7.49 (m, 2H), 7.48 – 7.42 (m, 7H), 7.39 – 7.34 (m, 3H), 7.18 – 7.05 (m, 5H). ^{13}C NMR (126 MHz, Methylene Chloride-d_2) δ 160.23, 159.03, 144.29, 142.34, 139.60, 138.47, 135.43, 133.26, 131.78, 130.14, 129.23, 128.87, 128.73, 128.18, 127.93, 127.76, 127.53, 127.17, 121.78 (q, -CF_3), 119.71. *Note: one carbon from the NTF_2^- anion is not visible due to high coupling and crowding in the aromatic region.* ^{19}F NMR (471 MHz, Methylene Chloride-d_2) δ -79.02 (Br). ^{11}B NMR (161 MHz, Methylene Chloride-d_2) δ 10.96. Elemental analysis calculated for $C_{27}H_{19}BF_6N_2O_4S_2$: C 51.94%, H 3.07%, N 4.49%, found C 51.38%, H 3.22%, N 4.39%. While the percentage of C is slightly outside the allowable limit for analytical purity, these values are provided to illustrate the best values obtained to date.

Synthesis of 6^H. To a solution of chloroborane $\mathbf{4^H}$ (150 mg, 0.395 mmol) in THF (10 ml), solid KC_8 (107 mg, 0.790 mmol) was added, causing the pale yellow solution to turn dark orange with the simultaneous formation of black graphite precipitate. This solution was stirred for 5 min and then filtered through a swivel frit apparatus. After volatiles were removed under vacuum, benzene (10 ml) was added, yielding an orange solid with a dark orange supernatant, which was filtered through the swivel-frit apparatus. The solid was washed several times with pentane (10 ml) and dried under vacuum yielding a bright orange solid $\mathbf{6^H}$ (60 mg, 0.156 mmol, 39%). Crystals suitable for X-ray diffraction were acquired through the addition of 0.16 mmol of 2,2,2-cryptand to a THF solution of $\mathbf{6^H}$, yielding single crystals at room temperature after one hour. ^{1}H NMR (500 MHz, Tetrahydrofuran-d_8) δ 7.77 (dd, J = 7.0, 1.3 Hz, 1H, Py-**H**), 7.59 – 7.51 (m, 2H), 7.23 – 7.16 (m, 2H), 7.15 – 7.04 (m, 5H, 1 Py-**H**), 7.04 – 6.95 (m, 3H), 6.94 – 6.87 (m, 1H), 6.78 (t, J = 7.7 Hz, 2H), 6.60 – 6.52 (m, 1H), 5.67 (ddd, J = 8.8, 5.9, 1.2 Hz, 1H, Py-**H**), 5.59 (ddd, J = 7.1, 5.7, 1.4 Hz, 1H, Py-**H**). ^{13}C NMR (126 MHz, Tetrahydrofuran-d_8; *note: carbons attached to boron not visible in NMR spectra*): δ 147.09, 142.19, 134.80, 131.16, 130.71, 128.01, 127.67, 127.58, 127.47, 127.11, 124.49, 122.83, 119.91, 118.97, 117.24, 108.73, 106.36. Elemental analysis calculated for $C_{25}H_{19}BKN$ C 78.33%, H 5.00%, N 3.65%, found C 78.45%, H 4.68%, N 3.34%.

Synthesis of 7^H•$B(C_6F_5)_4$.

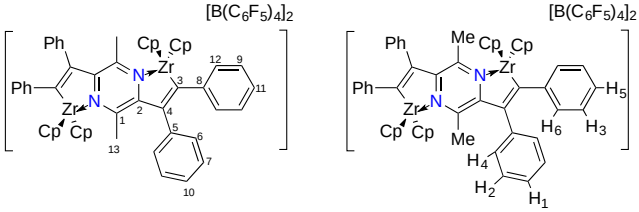

A solution of $Ph_3CB(C_6F_5)_4$ (1.10 g, 1.20 mmol) in PhCl (5.0 ml) was added drop-wise to a solution of dimethylzirconocene (300 mg, 1.20 mmol) in PhCl (5.0 ml) while stirring under an argon atmosphere on a swivel-frit apparatus. 2,5-dimethylpyrazine (65 mg, 0.60 mmol) in PhCl (1.0 ml) was then added drop-wise to the reaction mixture with stirring, turning the solution from dark brown colour to pale yellow and causing a yellow solid to precipitate: this mixture was stirred at room temperature for one hour. To this suspension, diphenylacetylene (214 mg, 1.20 mmol) in PhCl (5.0 ml) was added and the reaction was heated at 80 °C for 12 h, yielding a purple solution that upon cooling to room temperature precipitated a dark purple solid that was then filtered and rinsed several times with pentane (25 ml) to yield compound $\mathbf{7^H}$ as a dark purple solid (1.28 g, 0.57 mmol, 95%). Crystals suitable for X-ray diffraction analysis were grown through slow diffusion of pentane into a concentrated chlorobenzene solution of compound $\mathbf{7^H}$. ^{1}H NMR (500 MHz, Tetrahydrofuran-d_8) δ 7.27 (d, J = 1.7 Hz, 2H, $\mathbf{H_1}$), 7.26 (d, J = 2.1 Hz, 4H, $\mathbf{H_2}$), 7.15 (dd, J = 8.2, 7.4 Hz, 4H, $\mathbf{H_3}$), 7.08 – 7.03 (m, 4H, $\mathbf{H_4}$), 7.02 – 6.95 (m, 2H, $\mathbf{H_5}$), 6.85 (dd, J = 8.2, 1.3 Hz, 4H, $\mathbf{H_6}$), 6.69 (s, 20H, Cp-**H**), 0.95 (s, 6H, Me-**H**). ^{13}C NMR (126 MHz, Tetrahydrofuran-d_8) δ 151.55 (C1), 149.15(C2), 148.88 (dm, $B(C_6F_5)_4$), 145.70 (C3), 138.87 (dm, $B(C_6F_5)_4$), 138.59 (C4), 138.43 (C5), 136.78 (dm, $B(C_6F_5)_4$), 130.65 (C6), 129.51 (C7), 128.98 (C8), 128.89 (C9), 128.84 (C10), 126.50 (C11), 125.83 (C12), 124.90 (m, $B(C_6F_5)_4$), 117.52 (Cp), 22.72 (Me). Elemental analysis calculated for $C_{102}H_{46}B_2F_{40}N_2Zr_2$ C 54.12%, H 2.05%, N 1.24%, found C 53.79%, H 1.92%, N 1.19%.

Synthesis of 7^{tBu}•$B(C_6F_5)_4$. A solution of $Ph_3CB(C_6F_5)_4$ (2.121 g, 2.30 mmol) in PhCl (5.0 ml) was added dropwise to a solution of dimethylzirconocene (575 mg, 2.30 mmol) in PhCl (20 ml) with stirring under an argon atmosphere on a swivel-frit apparatus. 2,5-dimethylpyrazine (125 mg, 1.15 mmol) in PhCl (1.0 ml) was then added dropwise to the reaction mixture with stirring, turning the solution from dark brown to pale yellow and causing a yellow solid to precipitate. To this suspension, di(*p*-tBu-phenyl)acetylene (700 mg, 2.41 mmol) in PhCl (10 ml) was added and the reaction was heated at 80 °C for 12 h, yielding a purple solution that upon cooling precipitated a dark purple solid that was then filtered and rinsed several times with pentane (25 ml) to yield compound $\mathbf{7^{tBu}}$•$\mathbf{B(C_6F_5)_4}$ as a dark purple solid (1.75 g, 0.74 mmol, 64%). ^{1}H NMR (500 MHz, Tetrahydrofuran-d_8) δ 7.26 (d, J = 8.4 Hz, 4H), 7.16 (d, J = 8.5 Hz, 4H), 6.92 (d, J = 8.4 Hz, 4H), 6.72 (d, J = 8.4 Hz, 4H), 6.68 (s, 20H, Cp-**H**), 1.23 (s, 18H), 1.20 (s, 18H), 1.09 (s, 6H). ^{13}C NMR (126 MHz, Tetrahydrofuran-d_8) δ 152.17, 151.35, 149.54, 149.19, 148.87 (dm, $B(C_6F_5)_4$), 143.00, 138.86 (dm, $B(C_6F_5)_4$), 138.76, 136.81 (dm, $B(C_6F_5)_4$), 135.90, 130.33, 125.99, 125.84, 125.41, 124.82 (m, $B(C_6F_5)_4$), 117.28, 35.02, 34.71, 31.23, 31.21, 23.10. ^{19}F NMR (471 MHz, Tetrahydrofuran-d_8) δ –132.97 to –134.53 (m), –165.54 (t, J = 20.3 Hz), –169.13 (t, J = 19.1 Hz). Elemental analysis: calculated for $C_{118}H_{78}B_2F_{40}N_2Zr_2$: C 56.97%, H 3.16%, N 1.13%, Found: C 56.60%, H 3.22%, N 1.15%.

Synthesis of *cis/trans*-8^H: A 100 ml round-bottom flask was charged with $\mathbf{7^H}$•$\mathbf{B(C_6F_5)_4}$ (1.00 g, 0.423 mmol) and [nBu_4N][$PhBCl_3$] (0.370 g, 0.846 mmol). Under an argon atmosphere this was attached to a reflux condenser and 50 ml of DCM was vacuum-transferred at –78 °C; this mixture was allowed to warm to room temperature, and stirred for 2 h. Upon addition of dichloromethane and subsequent warming to room temperature, the dark purple solution turned pale yellow. The reaction was then heated at 50 °C for 12 h, during which the mixture turned a fluorescent pink. The product was then purified by silica gel chromatography using DCM:Hex (3:5), where a pink fraction was collected containing both the *cis* and *trans* isomers in a roughly 50:50 ratio, with a yield of 180 mg (60%). It was then possible to isolate near pure samples of each isomer through selective recrystallization. Crystals of mostly the *trans* isomer were grown through slow diffusion of hexanes (12 ml) into a solution of the isomers (100 mg) in DCM (8 ml). While mostly one isomer was crystallized it proved impossible in our hands to isolate completely pure *trans* form. When the supernatant of the recrystallization was placed in the –35 °C freezer for 4 days single crystals of approx. 98% of the *cis* isomer were formed. NMR data for only the *cis* isomer is listed, but ^{1}H spectra of the mixture is also given in Figure S18 in the Supporting Information. ^{1}H NMR (500 MHz, Methylene Chloride-d_2) δ 7.49 – 7.41 (m, 8H), 7.41 – 7.37 (m, 2H), 7.33 (td, J = 7.5, 1.6 Hz, 2H), 7.32 – 7.25 (m, 4H), 7.23 (t, J = 7.7 Hz, 2H), 7.10 – 7.04 (m, 2H), 7.03 (dd, J = 7.1, 1.5 Hz, 2H), 6.97 (td, J = 7.6, 1.7 Hz, 4H), 6.81 – 6.74 (m, 4H), 2.16 (s, 6H). 13C NMR (126 MHz, Methylene Chloride-d_2) δ 175.23 (br), 151.07, 147.19, 138.47 (br), 136.77, 134.86, 133.58, 131.02, 129.55, 129.46, 128.28, 128.02, 127.70, 127.56, 126.84, 126.76, 19.21. Elemental analysis of mixture of two isomers, calculated for $C_{46}H_{36}B_2Cl_2N_2$ C 77.89%, H 5.12%, N 3.95%, found: C 78.00%, H 5.42%, N 3.93%.

Synthesis of *cis/trans*-8^{tBu}. A 100 ml round-bottom flask was charged with $\mathbf{7^{tBu}}$•$\mathbf{B(C_6F_5)_4}$ (1.75 g, 0.740 mmol) and

[nBu_4N][$PhBCl_3$] (0.647 g, 1.40 mmol). Under an inert atmosphere this was attached to a reflux condenser and 50 ml of DCM was added at –78 °C; this mixture was allowed to warm to room temperature, and stirred for 2 h. Upon addition of dichloromethane the dark purple solution turned pale yellow. The reaction mixture was then heated at 50 °C for 12 h, during which the mixture turned a fluorescent purple, and formed some dark purple precipitate. After heating, the reaction mixture was filtered under atmospheric conditions to give a dark purple solid which was one of the two possible isomers (called here isomer a) in a yield of 210 mg (30%). The remaining supernatant from filtration was then purified through column chromatography using silica gel and DCM:Hex (3:1) to give mostly isomer b, with minor amounts of isomer a present in a yield of 160 mg (23%), and an overall yield for both isomer of 370 mg (53%). NMR data are given for isomer b, as it was the only one with high enough solubility to make characterization possible. ^{1}H NMR (500 MHz, Methylene Chloride-d_2) δ 7.53 (t, J = 6.7 Hz, 3H), 7.37 – 7.25 (m, 5H), 7.06 (d, J = 8.2 Hz, 1H), 7.02 (dd, J = 8.6, 1.7 Hz, 2H), 6.85 – 6.80 (m, 2H), 2.14 (d, J = 1.4 Hz, 3H), 1.35 (d, J = 1.7 Hz, 9H), 1.19 (d, J = 1.6 Hz, 9H). ^{13}C NMR (126 MHz, Methylene Chloride-d_2) δ 174.00 (br), 152.21, 151.89, 151.38, 147.97, 140.46 (br), 134.54, 134.07, 133.44, 131.99, 130.12, 129.62, 128.54, 127.60, 126.43, 124.76, 34.99, 34.75, 31.45, 31.17, 19.99. Elemental analysis of mixture of two isomers, calculated for $C_{62}H_{68}B_2Cl_2N_2$ C 79.75%, H 7.34%, N 3.00%, found: C 79.51%, H 7.36%, N 2.93%.

Synthesis of 9^{tBu}.

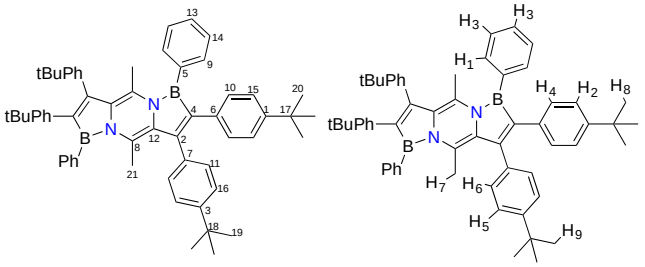

A 50 ml round-bottom flask was charged with *cis/trans*-**8^{tBu}** (80 mg, 0.086 mmol) in THF (15 ml), and KC_8 (23 mg, 0.17 mmol) was added the flask attached to a swivel-frit apparatus. Immediately upon addition of KC_8 the bright purple solution turned dark yellow. This mixture was stirred under an argon atmosphere for 1 hour and then filtered through the swivel-frit and washed with THF three times. Pentane (20 ml) was then vacuum-transferred into the swivel-frit apparatus and a yellow solid precipitated. This was filtered back through the frit, washed several times with pentane and all solvent removed in vacuo yielding a yellow solid (35 mg, 47%). Crystal suitable for X-ray diffraction analysis were grown through the slow diffusion of pentane into a concentrated THF solution of **9^{tBu}**. ^{1}H NMR (500 MHz, Tetrahydrofuran-d_8) δ 7.32 (dd, J = 6.3, 3.0 Hz, H_1, 4H), 7.27 (d, J = 7.9 Hz, H_2, 4H), 7.20 – 7.13 (m, H_3, 6H), 7.07 (d, J = 7.8 Hz, H_4, 4H), 6.85 (d, J = 8.1 Hz, H_5, 4H), 6.57 (d, J = 8.4 Hz, H_6, 4H), 1.64 (s, H_7, 6H), 1.26 (s, H_8, 18H), 1.12 (s, H_9, 18H). ^{13}C NMR (126 MHz, Tetrahydrofuran-d_8) δ 150.71 (C1), 150.02 (C2), 147.85 (C3), 146.56 (br, C4), 141.10 (br, C5), 136.48 (C6), 136.44 (C7), 132.65 (C8), 132.60 (C9), 130.13 (C10), 129.80 (C11), 129.46 (C12), 127.98 (C13), 127.78 (C14), 125.50 (C15), 124.14 (C16), 34.96 (C17), 34.56 (C18), 31.44 (C19), 31.41 (C20), 20.36 (C21). ^{11}B NMR (161 MHz, Tetrahydrofuran-d_8) δ 42.3. Elemental analysis, calculated for $C_{62}H_{68}B_2N_2$: C 86.30%, H 7.94%, N 3.25%, found: C 85.93%, H 7.85%, N 3.36%.

Computational details. All DFT calculations were performed with the Turbomole 7.1 program package.[76] Structures were optimized using BH-LYP[77-79] hybrid functional and Ahlrich's small triple-zeta valence quality def-TZVP basis sets.[80] Frequency calculations were performed to ascertain the nature of stationary points on the potential energy surface. Electronic excitation energies were calculated using the time-dependent density functional formalism (TDDFT) on optimized structures. The module mpshift[76] was used to calculate the nucleus independent chemical shifts (NICS)[81] and produce XDENS files that contain the one-particle densities and the magnetically perturbed densities in AO basis, required by the Gauge including magnetically induced current (GIMIC) analyses.[71-72] GIMIC analyses were calculated with the GIMIC program,[82] while figures of GIMIC surfaces were generated with the gOpenMol program.[83]

ASSOCIATED CONTENT

Supporting Information

The Supporting Information is available free of charge on the ACS Publications website.

Experimental and characterization details for all new compounds, including spectroscopic data, electrochemical data and X-ray crystallographic data. (PDF)
X-ray crystallographic data (CIF)
Cartesian coordinates for calculated structures (XYZ)

AUTHOR INFORMATION

Corresponding Author

- Email for W.E.P: wpiers@ucalgary.ca
- Email for J.M.R: j.mikko.rautiainen@jyu.fi

Notes

The authors declare no competing financial interest.

ACKNOWLEDGMENT

Funding for this work was provided by NSERC of Canada (Discovery Grant) the Canada Research Chair secretariat (Tier I CRC 2013–2020) to W. E. P. and the Academy of Finland (project #136929) and Emil Aaltonen Foundation to H. M. T. The Alexander von Humboldt Foundation (W. E. P.) is acknowledged for financial support. M. M. M. thanks NSERC of Canada for PGSD Scholarship support.

REFERENCES

1. Dewar, M. J. S.; Kubba, V. P.; Pettit, R., *J. Chem. Soc.* **1958**, 3073-3076.
2. The abstract of this initial paper in a series by Dewar et al. contains a highly succinct statement of the rationale for the "BN for CC" hypothesis: "Replacement of one carbon atom in an aromatic hydrocarbon by nitrogen gives rise to an isoconjugate positive ion; e.g., the pyridinium ion is related in this way to benzene. Replacement by boron should give an analogous negative ion. Replacement of a pair of carbon atoms, one by nitrogen and one by boron, should therefore give a neutral aromatic system."
3. Stock, A.; Pohland, E., *Ber. Dtsch. Chem. Ges.* **1926**, *59*, 2210-2215.
4. Bosdet, M. J. D.; Piers, W. E.; Sorensen, T. S.; Parvez, M., *Angew. Chem. Int. Ed.* **2007**, *46*, 4940-4943.
5. Emslie, D. J. H.; Piers, W. E.; Parvez, M., *Angew. Chem. Int. Ed.* **2003**, *42*, 1252-1255.
6. Jaska, C. A.; Emslie, D. J. H.; Bosdet, M. J. D.; Piers, W. E.; Sorensen, T. S.; Parvez, M., *J. Am. Chem. Soc.* **2006**, *128*, 10885-10896.
7. Neue, B.; Araneda, J. F.; Piers, W. E.; Parvez, M., *Angew. Chem. Int. Ed.* **2013**, *52*, 9966-9969.
8. Wang, X.-Y.; Narita, A.; Feng, X.; Müllen, K., *J. Am. Chem. Soc.* **2015**, *137*, 7668-7671.
9. Wang, X.; Zhang, F.; Liu, J.; Tang, R.; Fu, Y.; Wu, D.; Xu, Q.; Zhuang, X.; He, G.; Feng, X., *Org. Lett.* **2013**, *15*, 5714-5717.
10. Wang, X.-Y.; Zhuang, F.-D.; Wang, X.-C.; Cao, X.-Y.; Wang, J.-Y.; Pei, J., *Chem. Commun.* **2015**, *51*, 4368-4371.
11. Müller, M.; Maichle-Mössmer, C.; Bettinger, H. F., *Angew. Chem. Int. Ed.* **2014**, *53*, 9380-9383.
12. Muller, M.; Behnle, S.; Maichle-Mossmer, C.; Bettinger, H. F., *Chem. Commun.* **2014**, *50*, 7821-7823.

13. Ishibashi, J. S. A.; Marshall, J. L.; Mazière, A.; Lovinger, G. J.; Li, B.; Zakharov, L. N.; Dargelos, A.; Graciaa, A.; Chrostowska, A.; Liu, S.-Y., *J. Am. Chem. Soc.* **2014**, *136*, 15414-15421.
14. Wang, X. Y.; Zhang, F.; Schellharnmer, K. S.; Machata, P.; Ortmann, F.; Cuniberti, G.; Fu, Y. B.; Hunger, J.; Tang, R. Z.; Popov, A. A.; Berger, R.; Mullen, K.; Feng, X. L., *J. Am. Chem. Soc.* **2016**, *138*, 11606-11615.
15. Tasior, M.; Gryko, D. T., *J. Org. Chem.* **2016**, *81*, 6580-6586.
16. Huang, H. N.; Pan, Z. X.; Cui, C. M., *Chem. Commun.* **2016**, *52*, 4227-4230.
17. Baggett, A. W.; Guo, F.; Li, B.; Liu, S.-Y.; Jäkle, F., *Angew. Chem. Int. Ed.* **2015**, *54*, 11191-11195.
18. Wan, W.-M.; Baggett, A. W.; Cheng, F.; Lin, H.; Liu, S.-Y.; Jakle, F., *Chem. Commun.* **2016**, *52*, 13616-13619.
19. Wang, X.-Y.; Zhuang, F.-D.; Wang, J.-Y.; Pei, J., *Chem. Commun.* **2015**, *51*, 17532-17535.
20. Zhao, R. Y.; Dou, C. D.; Xie, Z. Y.; Liu, J.; Wang, L. X., *Angew. Chem. Int. Ed.* **2016**, *55*, 5313-5317.
21. Hatakeyama, T.; Hashimoto, S.; Seki, S.; Nakamura, M., *J. Am. Chem. Soc.* **2011**, *133*, 18614-18617.
22. Wang, X.-Y.; Yang, D.-C.; Zhuang, F.-D.; Liu, J.-J.; Wang, J.-Y.; Pei, J., *Chem. Eur. J.* **2015**, *21*, 8867-8873.
23. Wang, S. N.; Yang, D. T.; Lu, J. S.; Shimogawa, H.; Gong, S. L.; Wang, X.; Mellerup, S. K.; Wakamiya, A.; Chang, Y. L.; Yang, C. L.; Lu, Z. H., *Angew. Chem. Int. Ed.* **2015**, *54*, 15074-15078.
24. Wang, X.-Y.; Zhuang, F.-D.; Wang, R.-B.; Wang, X.-C.; Cao, X.-Y.; Wang, J.-Y.; Pei, J., *J. Am. Chem. Soc.* **2014**, *136*, 3764-3767.
25. Wang, X.-Y.; Zhuang, F.-D.; Zhou, X.; Yang, D.-C.; Wang, J.-Y.; Pei, J., *J. Mater. Chem. C* **2014**, *2*, 8152-8161.
26. Krieg, M.; Reicherter, F.; Haiss, P.; Ströbele, M.; Eichele, K.; Treanor, M.-J.; Schaub, R.; Bettinger, H. F., *Angew. Chem. Int. Ed.* **2015**, *54*, 8284-8286.
27. Knack, D. H.; Marshall, J. L.; Harlow, G. P.; Dudzik, A.; Szaleniec, M.; Liu, S.-Y.; Heider, J., *Angew. Chem. Int. Ed.* **2013**, *52*, 2599-2601.
28. Liu, L.; Marwitz, A. J. V.; Matthews, B. W.; Liu, S.-Y., *Angew. Chem. Int. Ed.* **2009**, *48*, 6817-6819.
29. Molander, G. A.; Wisniewski, S. R.; Amani, J., *Org. Lett.* **2014**, *16*, 5636-5639.
30. Molander, G. A.; Amani, J.; Wisniewski, S. R., *Org. Lett.* **2014**, *16*, 6024-6027.
31. Lee, H.; Fischer, M.; Shoichet, B. K.; Liu, S.-Y., *J. Am. Chem. Soc.* **2016**, *138*, 12021-12024.
32. Bosdet, M. J. D.; Piers, W. E., *Can. J. Chem.* **2009**, *87*, 8-29.
33. Campbell, P. G.; Marwitz, A. J. V.; Liu, S.-Y., *Angew. Chem. Int. Ed.* **2012**, *51*, 6074-6092.
34. Wang, X.-Y.; Wang, J.-Y.; Pei, J., *Chem. Eur. J.* **2015**, *21*, 3528-3539.
35. Morgan, M. M.; Piers, W. E., *Dalton Trans.* **2016**, *45*, 5920-5924.
36. Helten, H., *Chem.-Eur. J.* **2016**, *22*, 12972-12982.
37. Liu, Z.; Marder, T. B., *Angew. Chem. Int. Ed.* **2008**, *47*, 242-244.
38. Abbey, E. R.; Liu, S. Y., *Org. Biomol. Chem.* **2013**, *11*, 2060-2069.
39. Ishida, N.; Narumi, M.; Murakami, M., *Org. Lett.* **2008**, *10*, 1279-1281.
40. Yuan, K.; Suzuki, N.; Mellerup, S. K.; Wang, X.; Yamaguchi, S.; Wang, S., *Org. Lett.* **2016**, *18*, 720-723.
41. Hafner, K.; Stowasser, B.; Krimmer, H.-P.; Fischer, S.; Böhm, M. C.; Lindner, H. J., *Angew. Chem. Int. Ed. Engl.* **1986**, *25*, 630-632.
42. Nendel, M.; Goldfuss, B.; Houk, K. N.; Hafner, K., *J. Mol. Struct. Theochem.* **1999**, *461–462*, 23-28.
43. Tobe, Y., *Chemical Record* **2015**, *15*, 86-96.
44. Frederickson, C. K.; Zakharov, L. N.; Haley, M. M., *J. Am. Chem. Soc.* **2016**, *138*, 16827-16838.
45. Fan, C.; Piers, W. E.; Parvez, M., *Angew. Chem. Int. Ed.* **2009**, *48*, 2955-2958.
46. Houghton, A. Y.; Karttunen, V. A.; Piers, W. E.; Tuononen, H. M., *Chem. Commun.* **2014**, *50*, 1295-1298.
47. Jordan, R. F.; Taylor, D. F., *J. Am. Chem. Soc.* **1989**, *111*, 778-779.
48. Guram, A. S.; Jordan, R. F., *Organometallics* **1991**, *10*, 3470-3479.
49. Jordan, R. F.; Guram, A. S., *Organometallics* **1990**, *9*, 2116-2123.
50. Chien, J. C. W.; Tsai, W. M.; Rausch, M. D., *J. Am. Chem. Soc.* **1991**, *113*, 8570-8571.
51. Jordan, R. F.; Guram, A. S., *Organometallics* **1990**, *9*, 2116-2123.
52. Montavon, T. J.; Türkmen, Y. E.; Shamsi, N. A.; Miller, C.; Sumaria, C. S.; Rawal, V. H.; Kozmin, S. A., *Angew. Chem. Int. Ed.* **2013**, *52*, 13576-13579.
53. Antoniotti, S.; Dalla, V.; Duñach, E., *Angew. Chem. Int. Ed.* **2010**, *49*, 7860-7888.
54. Luinstra, G. A., *J. Organomet. Chem.* **1996**, *517*, 209-215.
55. Sheikh, S. U., *J. Therm. Anal.* **1980**, *18*, 299-306.
56. For related BN-fluorene systems see references 55 and 56.
57. Ishida, N.; Moriya, T.; Goya, T.; Murakami, M., *J. Org. Chem.* **2010**, *75*, 8709-8712.
58. Shaikh, A. C.; Ranade, D. S.; Thorat, S.; Maity, A.; Kulkarni, P. P.; Gonnade, R. G.; Munshi, P.; Patil, N. T., *Chem. Commun.* **2015**, *51*, 16115-16118.
59. Piers, W. E.; Bourke, S. C.; Conroy, K. D., *Angew. Chem. Int. Ed.* **2005**, *44*, 5016-5036.
60. Wang, C. C.; Tang, T. H.; Wu, L. C.; Wang, Y., *Acta Cryst. Sect. A* **2004**, *60*, 488-493.
61. Dunitz, B. J. D.; Kriiger, C.; Irngartinger, H.; Maverick, E. F.; Wang, Y.; Nixdorf, M., *Angew. Chem. Int. Ed. Engl.* **1988**, *27*, 387-389.
62. Hertwig, R. H.; Holthausen, M. C.; Koch, W.; Maksic, Z. B., *Angew. Chem. Int. Ed.* **1994**, *33*, 1192-1194.
63. Moroni, L.; Gellini, C.; Salvi, P. R., *J. Mol. Struct. Theochem.* **2004**, *677*, 1-5.
64. Hafner, K.; Krimmer, H.-P., *Angew. Chem. Int. Ed. Engl.* **1980**, *19*, 199-201.
65. Bachmann, R.; Gerson, F.; Gescheidt, G.; Hafner, K., *Mag. Res. Chem.* **1995**, *33*, S60-S65.
66. Cary, D. R.; Green, J. C.; O'Hare, D., *Angew. Chem. Int. Ed.* **1997**, *36*, 2618-2620.
67. Bheemireddy, S. R.; Ubaldo, P. C.; Rose, P. W.; Finke, A. D.; Zhuang, J. P.; Wang, L. C.; Plunkett, K. N., *Angew. Chem. Int. Ed.* **2015**, *54*, 15762-15766.
68. Rose, B. D.; Sumner, N. J.; Filatov, A. S.; Peters, S. J.; Zakharov, L. N.; Petrukhina, M. A.; Haley, M. M., *J. Am. Chem. Soc.* **2014**, *136*, 9181-9189.
69. A formally 16 p B4N8 s-indacene framework has been reported, but here we target BN s-indacenes that retain the 12 p electron count of the parent hydrocarbon.
70. Ly, H. V.; Tuononen, H. M.; Parvez, M.; Roesler, R., *Chem. Commun.* **2007**, 4522-4524.
71. Jusélius, J.; Sundholm, D.; Gauss, J., *J. Chem. Phys.* **2004**, *121*, 3952-3963.
72. Fliegl, H.; Taubert, S.; Lehtonen, O.; Sundholm, D., *PCCP* **2011**, *13*, 20500-20518.
73. Analysis of II_D2h ws further complicated by its diradical character and the lack of implementation for NMR parameter calculations that use unrestricted DFT formalism in Turbomole.
74. Marwitz, A. J. V.; Matus, M. H.; Zakharov, L. N.; Dixon, D. A.; Liu, S.-Y., *Angew. Chem. Int. Ed.* **2009**, *48*, 973-977.
75. Ghosh, D.; Periyasamy, G.; Pati, S. K., *PCCP* **2011**, *13*, 20627-20636.
76. TURBOMOLE V7.1 2016, a development of University of Karlsruhe and Forschungszentrum Karlsruhe GmbH, 1989-2007, TURBOMOLE GmbH, since 2007; available from http://www.turbomole.com
77. Becke, A. D., *Phys. Rev. A* **1988**, *38*, 3098-3100.
78. Lee, C.; Yang, W.; Parr, R. G., *Phys. Rev. B* **1988**, *37*, 785-789.
79. Becke, A. D., *J. Chem. Phys.* **1993**, *98*, 1372-1377.
80. Schaefer, A.; Huber, C.; Ahlrichs, R., *J. Chem. Phys.* **1994**, *100*, 5829-5835.

81. Schleyer, P. v. R.; Maerker, C.; Dransfeld, A.; Jiao, H.; Hommes, N. J. R. v. E., *J. Am. Chem. Soc.* **1996**, *118*, 6317-6318.
82. GIMIC program, version 2.1.4, Juselius, J., University of Tromsø, 2003-2011.
83. Bergman, D. L.; Laaksonen, L.; Laaksonen, A., *J. Mol. Graph. Model.* **1997**, *15*, 301-306.

Synopsis: A method for the preparation of 1,5-dibora-4a,8a-diaza-*s*-indacenes allows for a comparison of properties with the all carbon *s*-indacene molecule.